

PHYSICAL REVIEW B

CONDENSED MATTER

THIRD SERIES, VOLUME 46, NUMBER 20

15 NOVEMBER 1992-II

X-ray-scattering determination of the dynamic structure factor of Al metal

P. M. Platzman, E. D. Isaacs, and H. Williams
AT&T Bell Laboratories, Murray Hill, New Jersey 07974

P. Zschack
Oak Ridge Associated Universities, Brookhaven National Laboratory, Upton, New York 11973

G. E. Ice
Oak Ridge National Laboratories, Oak Ridge, Tennessee 37831
(Received 13 May 1992)

The dynamic structure factor $S(\mathbf{q}, \omega)$ of conduction electrons in single-crystal Al has been measured using 5.66-keV synchrotron x radiation with 1.5-eV energy resolution. These measurements confirm the existence of strong non-random-phase-approximation-like correlations in an electron liquid where band-structure effects are unimportant.

Perhaps the most extensively studied true many-body system is the interacting electron gas in the presence of a uniform positive background (jellium).¹ For low temperatures, the parameter $r_s = (3/4\pi n)^{1/3} me^2/\hbar^2 \cong \langle V \rangle / \langle KE \rangle$ (n is the electron density, and V and KE are the electron potential and kinetic energy, respectively) is larger than unity, and there is no systematic method for quantitatively computing the properties of this system. This is particularly true for the finite wave vector ($q \sim q_F$, the Fermi wave vector) and finite frequency ($\omega \sim \omega_F$) response functions.² Despite enormous theoretical work there have been surprisingly few experimental results on appropriate model systems. Transport and light-scattering experiments probe $q \simeq 0$ while high-energy transmission e^- -beam experiments are effectively limited to $q < q_F$.³ The only practical technique currently available for studying finite q is inelastic x-ray scattering.^{4,5}

For x rays in the 5–10-keV range and for scattering from any of the light elements $Z < 25$ the inelastic x-ray-scattering cross section is given by⁴

$$\frac{d\sigma}{d\Omega d\omega} = (\mathbf{e}_0 \cdot \mathbf{e}_1)^2 r_0^2 \left(\frac{\omega_1}{\omega_0} \right) S(\mathbf{q}, \omega), \quad (1)$$

where (\mathbf{e}_0, ω_0) and (\mathbf{e}_1, ω_1) are the polarization and frequency of the incident and scattered photon, respectively, and r_0 is the classical electron radius. $S(\mathbf{q}, \omega)$ is the dynamic structure factor which is given by

$$S(\mathbf{q}, \omega) = \frac{1}{\phi_q} \text{Im} \epsilon(\mathbf{q}, \omega)^{-1}, \quad (2)$$

where the complex dielectric response function $\epsilon(\mathbf{q}, \omega)$ is

a matrix in band indices, and $\phi_q = 4\pi e^2/q^2$ is the Fourier transform of the electrostatic potential energy e^2/r . For x-ray scattering, the whole range of q is experimentally accessible and current techniques allow energy resolution ΔE in the fraction of an eV range. However, despite its suitability, inelastic x-ray-scattering experiments have had limited success in quantifying the properties of the finite wave-vector dielectric response function of solids. This is primarily due to the need for brighter x-ray sources and more efficient spectrometers.⁵

Despite these experimental problems, Platzman and Eisenberger (PE) (Ref. 6) published several papers on the dynamic structure factor $S(\mathbf{q}, \omega)$ of several light solids, Li, graphite, Be, and Al in the regime ($q \simeq q_F$, $0 < \omega < 2\omega_F$). These experiments had good q resolution and an energy resolution of several (roughly three) electron volts. The measurements revealed several interesting features of the dynamic structure of the electron liquid in these “metals.” They observed that in the region $q_F < q < 2q_F$ the excitation spectrum had much more weight at lower frequency than predicted by mean-field theory, which is often called the random-phase approximation (RPA) or even simple exchange modified RPA.⁷ The shape of the spectrum was also anomalous. At $q/q_F \simeq 1.5$, for example, it had a double humped structure, the lower bump being much sharper in graphite and Be than in Al. At that time PE argued that these features in such diverse systems were manifestations of the complex dynamical behavior of the electron liquid immersed in jellium and that band-structure effects were to a rough approximation unimportant on this energy ($E \geq 20$ eV) and momentum ($q \geq q_F$) scale.

Since that time Schulke and co-workers⁸ have performed an extensive and rather beautiful set of high-resolution ($\Delta E \cong 1$ eV) measurements on Be metal. In these experiments they were able to show conclusively that band structure (nonjellium background) played a very important role. However they too were forced to include many-body effects beyond simple RPA in their fit to the data. There is no question that Be is less free-electron-like than Al and while band structure does play a significant role in Be, it is unlikely that it could play an important role in Al at $\omega/\omega_F \cong 2$. This left open the possibility that there are interesting correlation effects in $S(\mathbf{q}, \omega)$ for jelliumlike aluminum at $r_s = 2$.

In this paper we report additional measurements of the dynamic structure factor, $S(\mathbf{q}, \omega)$, for a single crystal of high purity aluminum. The spectra were taken at the Oak Ridge National Laboratory beamline X14 at the National Synchrotron Light Source at Brookhaven National Laboratory. The energy of the incident beam was tuned to 5.66 keV with a full width at half maximum (FWHM) of approximately 1 eV as determined by a Si(111) monochromator and a set of vertical collimating slits. The thickness of the Al sample was one-half of an x-ray-absorption length ($\sim 25 \mu\text{m}$) so that the measurements could be carried out in a transmission geometry. X-ray absorption strongly limits the effective sample volume illumination and hence the resulting inelastic scattering signal. For this reason, previous studies have been limited to light materials such as Be, Li, and graphite (Gr).^{5,6} The scattered radiation was collected and analyzed by a cylindrically bent, 5-cm axial \times 7.5-cm tangential graphite crystal with a 500-mm radius of curvature. The cylindrical axis was in the vertical scattering plane and was chosen as the dispersive direction so that, when used in conjunction with a position-sensitive proportional counter, a one-to-one parafocusing of the source (illuminated sample volume) onto the detector was achieved. In this configuration an 80-eV bandpass of radiation was collected into a well-defined angle of $\theta = 78 \pm 2^\circ$ for the Gr(006) reflection with a mosaic spread of 0.4° . The resolution of the scattering experiment was determined by the width of the elastic scattering peak (see Fig. 1) and was found to be about 1.5 eV. The energy resolution was limited by the thickness ($\sim 5000 \text{ \AA}$) of the mosaic blocks along the c axis ($\delta E/E = 1/x$, where x is the number of atomic layers in a single mosaic block) of the graphite. The response function of the analyzer-detector combination as a function of scattered energy was determined by scanning the input energy and measuring the intensity of the elastic peak for fixed analyzer angle. A similar analyzer-detector system was described elsewhere.⁹ Details of our system will be published.¹⁰ The data in Figs. 1 and 2 have been normalized to the measured analyzer-detector response. Typical collection times were about 5–6 h per spectrum. For example, for $q/q_F = 1.4$ (see Fig. 1), we obtained 4000 counts for about 1% statistics in the peak of the plasmon in 5 h.

The energy-loss spectrum at $q/q_F = 0.5$, shown in Fig. 1(a), shows a sharp plasmon peak near $\hbar\omega/\hbar\omega_F = 1.5$ ($\hbar\omega = 17$ eV and $\hbar\omega_F = 11.63$ eV) with a FWHM of 2.6 eV. The single particle continuum is observed at lower

energies. The spectrum shows features similar to the RPA results. RPA is shown by the solid line in Fig. 1(a), which has been broadened with the resolution function (elastic line) and the plasmon width is broadened an additional 0.6 eV to account for non-RPA-like damping. In addition, we picked a zero-momentum plasmon energy,

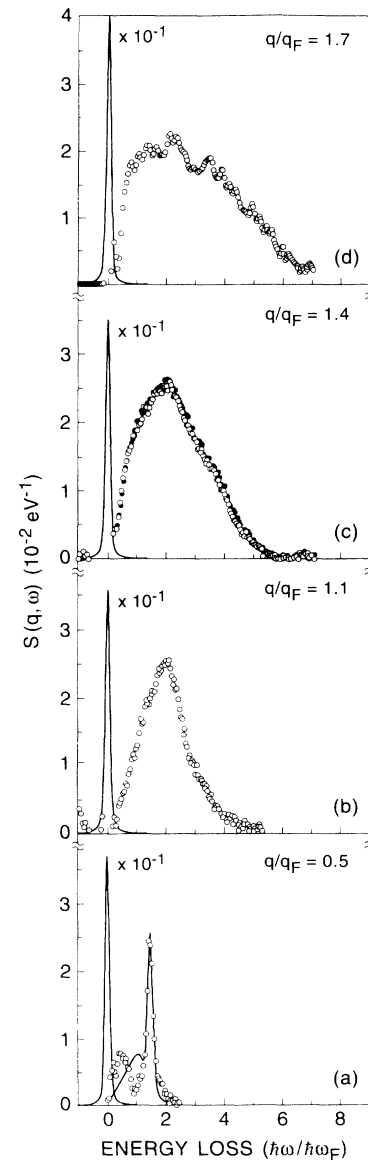


FIG. 1. $S(\mathbf{q}, \omega)$ for single-crystal aluminum for q parallel to the $\langle \frac{1}{2}, \frac{3}{2}, 0 \rangle$ axis. (a) $q/q_F = 0.5$. The solid line is RPA, broadened by a convolution with the measured resolution function (elastic line) and with the plasmon peak broadened by an additional 0.6 eV and shifted down by non-RPA corrections as described in the text. (b) $q/q_F = 1.1$; (c) $q/q_F = 1.4$ for q parallel to the $\langle \frac{1}{2}, \frac{3}{2}, 0 \rangle$ -axis (open circles) and tilted by approximately 10° from this axis (filled circles). Note the indistinguishability of these two spectra. (d) $q/q_F = 1.7$. The experimental resolution is given by the width of the elastic peak and is plotted in each spectrum and measured to be approximately 1.5 eV. Note: $\hbar\omega_F = 11.63$ eV and $q_F = 1.75 \text{ \AA}^{-1}$.

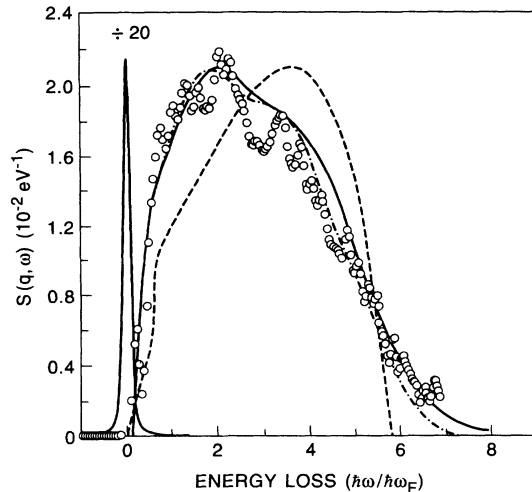


FIG. 2. $S(q, \omega)$ for $q/q_F = 1.7$ (open circles) compared with the two particle-hole pair theory due to Mukhopadhyay *et al.* (solid line) for $q/q_F = 1.6$ (Ref. 11). Also included are the RPA theory (dashed line) as well as the earlier data of PE (dash-dotted line) (Ref. 6) for $q/q_F = 1.6$.

$\hbar\omega_p$, of 15.3 eV with an exchange softened dispersion of the plasmon differing from its RPA value by a factor of 0.65, i.e., $\omega(q) = \omega_p \{1 + \alpha(qv_F/\omega_p)^2\}$, with $\alpha = 0.65\alpha_{\text{RPA}}$ ($\alpha_{\text{RPA}} = 0.3$) in agreement with previous measurements (see, for example, Ref. 3). Finally, although the overall shape and integrated weight of the single-particle excitations are in agreement with RPA, we note that the energy cutoff, which should be at $\hbar\omega/\hbar\omega_F = 1.25$, does not seem to agree. This was a surprise to us and although we do not understand the discrepancy it certainly merits further investigation.

The spectrum at $q/q_F = 1.1$ [Fig. 1(b)] is in sharp disagreement with RPA results. The entire spectrum is, as in PE, shifted to lower energies with a broad peak around $\hbar\omega/E_F = 2.58$ clearly in evidence. In addition, there is a definite shoulder in the neighborhood of $\hbar\omega/E_F = 3.44$. In Fig. 1(c) we show two sets of data taken at $q/q_F = 1.4$ for \mathbf{q} along two different crystal directions. The curves are identical within statistical uncertainty, i.e., there is no evidence for band-structure effects for angular changes of order 10° , in contrast, for example, to Be. Aluminum, unlike Be, is truly jelliumlike. The spectrum itself shows that the shoulder at $\hbar\omega/E_F = 3.45$ has increased in weight relative to the broad peak near $\hbar\omega/E_F = 2.6$. Continuing to a higher momentum transfer of $q/q_F = 1.7$ [Fig. 1(d)] the intensity of the high-energy shoulder increases into a bump and begins to dominate the spectrum. At still higher momentum transfers we expect that the high-energy bump will evolve smoothly into the Compton peak.

Almost all theories of these response functions start with some form of the RPA. The standard RPA (Ref. 1) is the leading term in a perturbation theory to order r_s .

In a diagrammatic expansion it consists of summing bubbles. The bubbles, or polarizability, are made up of single noninteracting particle-hole pairs, associated with the excitation of an electron from below to above the Fermi energy. The particle-hole pairs do not interact with each other (vertex corrections) or with the rest of the electrons (self-energy). This implies in a very straightforward fashion that only single particle-hole pairs may be excited in a single scattering event. In the intervening years, since the experiments of PE, there have been several serious theoretical attempts made to understand the observed structure.^{11,12} These theoretical analyses were based on modifications to the standard RPA. While we cannot discuss these theories in detail it is safe to say that the physics which gave roughly the correct behavior was the inclusion of a realistic self-energy $\Sigma(\mathbf{p}, \omega)$ in the propagators used in calculating the RPA polarizability (dielectric function). This formal procedure allows the possibility that two particle-hole pairs can be excited in the scattering process. The presence of two pairs and the associated expanded phase space allows for momentum conservation and permits many more low-lying excitations to be accessed. For example, if one of the pairs in the two particle-hole pair states has low momentum (the other one picks up the large q) then that pair excitation can look a bit like a plasmon giving a broad peak in the region of the zero-momentum plasmon. Of course, the theory takes all possible final states, matrix elements, etc., into account in a way which does not violate sum rules, etc. Although the aforementioned vertex corrections and larger numbers of pairs are neglected in these theories, none of these corrections are expected to change the scattering behavior quantitatively. In our opinion the most successful of these theories¹¹ showed that for jellium, at an $r_s = 2$ corresponding to Al, and at a $q/q_F = 1.6$ that there were two rather broad bumps. This theory along with the RPA theory, an exchange modified version of the RPA theory⁷ (without two pairs), the low-resolution (poor statistics) data of PE, and the current data at $q/q_F = 1.7$, is shown in Fig. 2. The peak intensity of the two particle-hole pair theory has been adjusted to fit our data.

The good semiquantitative agreement between the calculations of Ref. 12 and both spectra indicates that the inclusion of the self-energy into the RPA framework correctly describes the physical processes involved. In other words, multipair interactions supply the appropriate damping for the plasmon at low q and the necessary momentum and energy conservation at intermediate q to account for the double hump structure. In detail there are differences.

It is clear from the data presented in this report that further work at existing synchrotron sources can provide us with more insight into the behavior of the interacting electron gas. At small q the plasmon line is nearly resolution limited so that a reduction in resolution by a factor of 5, i.e., a few tenths of an eV, could reveal very significant information. With improved resolution it also seems important to carefully examine the single particle piece, for example, at $q/q_F \approx 0.5$ because this piece looks very different from the predicted RPA shape. Above all,

higher photon flux is needed. This would enable us to improve the energy resolution and access a broader range of q while maintaining the same or better statistics. Such improved flux will become available with the commissioning of beamline X21 at the National Synchrotron Light Source and with the completion of the European Synchrotron Radiation Facility and APS synchrotron facilities. Finally, a study of other model jellium systems like Na and K ($r_s \cong 4$) will allow us to probe the many-body aspects in further detail. Since K has a higher Z , and thus more absorption, this will be an experiment which requires the highest flux available. Such additional experimental data will allow modification of the theory and provide insights into the mechanisms underlying

short-range dynamical correlation effects in a real Fermi liquid.

We would like to thank Professor S. Schultz for supplying us with the crystal of Al. Thanks are also due Mitch Nelson for enlightening conversations and George Wright for his expert technical assistance. Oak Ridge National Laboratory beamline X14 at the National Synchrotron Light Source at Brookhaven National Laboratory is supported in part by the Division of Materials Sciences and Division of Chemical Sciences, U.S. Department of Energy under Contract No. DE-AC05-84OR21400 with the Martin Marietta Energy Systems, Inc.

¹G. D. Mahan, *Many Particle Physics* (Plenum, New York, 1983); D. Pines, *Elementary Excitations in Solids* (Benjamin, Massachusetts, 1983).

²At low frequencies and wave numbers the Landau Fermi-liquid theory provides a good phenomenological description of the excitation spectrum. For a good description of these ideas see D. Pines and P. Nozieres, *The Theory of Quantum Liquids* (Benjamin, New York, 1966).

³H. Raether, in *Springer Tracts in Modern Physics Vol. 38*, edited by G. Hohler (Springer, Berlin, 1965), p. 85.

⁴M. Blume, *J. Appl. Phys.* **57**, 3619 (1985); P. M. Platzman, *ibid.* **57**, 3623 (1985); *Momentum Distributions*, edited by R. Silver and P. Sokol (Plenum, New York, 1989).

⁵W. Schulke, *Nucl. Instrum. Methods A* **280**, 338 (1989); W. Schulke *et al.*, *Phys. Rev. B* **33**, 6744 (1986).

⁶P. M. Platzman and P. Eisenberger, *Phys. Rev. Lett.* **33**, 152 (1974); P. Eisenberger, P. M. Platzman, and P. Schmidt, *ibid.* **34**, 18 (1974); P. Eisenberger and P. M. Platzman, *Phys. Rev. B* **13**, 934 (1976).

⁷P. Vashista and K. S. Singwi, *Phys. Rev. B* **6**, 875 (1972).

⁸W. Schulke, H. Nagagawa, S. Mourikis, and A. Kaprolat, *Phys. Rev. B* **40**, 12 215 (1989).

⁹G. E. Ice and C. J. Sparks, Jr., *Nucl. Instrum. Methods A* **291**, 110 (1990).

¹⁰E. D. Isaacs, P. Zschack, P. M. Platzman, G. E. Ice, and D. W. Berreman (unpublished).

¹¹F. Green, D. Neilson, and J. Szymansky, *Phys. Rev. B* **31**, 2779 (1985); **31**, 2796 (1985); **31**, 5837 (1985).

¹²G. Mukhopadhyay, R. K. Kalia, and K. S. Singwi, *Phys. Rev. Lett.* **34**, 950 (1975).